

Article

Comparative Assessment of the Spatiotemporal Dynamics and Driving Forces of Natural and Constructed Wetlands in Arid and Semiarid Areas of Northern China

Jian Zhang [†] , Yao Qin [†], Yuxuan Zhang, Xin Lu and Jianjun Cao ^{*}

College of Geography and Environmental Science, Northwest Normal University, Lanzhou 730070, China; jianzhang@nwnu.edu.cn (J.Z.); 2021212884@nwnu.edu.cn (Y.Q.); 2021212893@nwnu.edu.cn (Y.Z.); 2021212899@nwnu.edu.cn (X.L.)

^{*} Correspondence: caojj@nwnu.edu.cn

[†] These authors contributed equally to this work.

Abstract: Arid and semiarid wetlands, the core geographical unit of desert oases, significantly benefit and improve the ecological environment. In this study, we systematically compared the spatiotemporal dynamics and driving forces of natural and constructed wetlands in arid and semiarid regions of northern China from 1995 to 2019. For these comparisons, we utilized a land-use transition matrix, partial least-squares–structural equation model (PLS-SEM), and geographically weighted regression (GWR) model. The results showed that (1) the area of wetlands as a whole showed an upward trend, with natural and constructed wetlands increasing by 4.16% and 11.86%, respectively. The increases mainly resulted from conversions of grassland and other lands (shrub, sparse vegetation, and bare land). (2) The direct dominant factors that drove natural wetland changes were soil and terrain, while those that drove constructed wetlands were human disturbances. Human disturbance, by affecting soil, had a higher significant indirect effect on natural wetlands. Heat, by affecting moisture, had the greatest indirect effect on constructed wetlands. (3) The sensitivity of natural and constructed wetlands to the responses of different drivers showed significant spatial heterogeneity. This study explores the interaction and driving mechanisms of human and natural attributes on natural and constructed wetlands and provides a scientific foundation for the restoration and sustainable development of wetlands in arid and semiarid areas.

Keywords: wetland pattern; natural and anthropogenic factors; land-use change; PLS-SEM; GWR



Citation: Zhang, J.; Qin, Y.; Zhang, Y.; Lu, X.; Cao, J. Comparative Assessment of the Spatiotemporal Dynamics and Driving Forces of Natural and Constructed Wetlands in Arid and Semiarid Areas of Northern China. *Land* **2023**, *12*, 1980. <https://doi.org/10.3390/land12111980>

Academic Editors: Zhenguo Niu, Bin Zhao, Zhaoqing Luan and Bo Guan

Received: 27 September 2023
Revised: 20 October 2023
Accepted: 25 October 2023
Published: 26 October 2023



Copyright: © 2023 by the authors. Licensee MDPI, Basel, Switzerland. This article is an open access article distributed under the terms and conditions of the Creative Commons Attribution (CC BY) license (<https://creativecommons.org/licenses/by/4.0/>).

1. Introduction

Wetlands comprise unique natural syntheses and complex land and water ecosystems; hence, they are one of the most important animal habitats and ecological landscapes on earth [1]. Wetlands supply a series of vital ecosystem services, such as climate regulation, freshwater retention, material production, flood control and water storage, carbon fixation and storage, water decontamination, and biodiversity maintenance [2,3]. The shrinkage and disappearance of wetlands in recent times is indisputable [4]; according to some related studies, over 50% of wetlands worldwide have transformed, degraded, or disappeared over the past 150 years [5,6]. Despite the introduction of several protection policies, such as the Ramsar Convention (an international treaty on wetland protection), the European Habitat Directive and the Wetlands International global organization [7], existing wetlands are still deteriorating [8]. Therefore, to inform future wetland management strategies and ecological protection, the patterns and dynamics of wetlands should be quantitatively assessed and the underlying drivers of change in wetlands should be further explored.

Natural factors and human activities are typically recognized the primary drivers of wetland destruction [9]. Not only has rapid urban expansion invaded large areas of wetlands, dams, highways, drainage canals, and other construction activities have also

disturbed hydrological patterns within wetlands [10]. Meanwhile, with the expansion of the population, growing numbers of wetlands are being drained by human actions, and the conflict between wetland protection and agricultural development is prominent. Among these factors, wetland drainage to create dryland farmland is the most common cause of natural wetland loss [11]. Climate change is altering the hydrological cycle, thereby damaging wetland functions via drought, flood, rising temperature, and increasing evapotranspiration [12]. Generally, soil quality is an important indicator of wetland ecosystem health [13]. Soil texture, pH, and other related soil quality indexes affect primary plant productivity and the nutrient cycle, and thus change the distribution of wetlands [14]. Terrain factors, such as elevation and slope, play an essential role in controlling the evolution of wetlands. Wetlands typically move to low altitudes over time [15]. Wetland plants, the primary producers of wetlands, interact with the abiotic environment (e.g., soil and hydrology) and other wetland organisms, thus significantly affecting how wetlands function [16]. The driving factors affecting wetland patterns are complex and variable. Thus, quantifying the respective contribution of every factor and its impacts on wetland patterns is challenging.

Currently, several aspects dominate research on the drivers of wetland change. First, many studies use remote sensing images to monitor the impact of land-use/cover change on wetlands [17–19]. Most of these studies concentrate on the dynamism of wetland area changes and cannot effectively quantify the contributing factors to this phenomenon. Second, other studies analyze wetland changes from specific perspectives, such as climate change [20], environmental pollution [21], and hydrological changes [22]. These studies often explore only one aspect of the causes of wetland changes. Finally, wetland ecological risk assessment systems are constructed to reveal the driving mechanisms of wetland change [23,24]. This kind of assessment is more focused on the possible risks posed to wetlands by a range of potential threats, including anthropogenic factors and natural hazards. The results of the above studies do not reflect the interactions between various driving forces, and a scientific evaluation of wetland changes from an integrated perspective is needed. The partial least-squares–structural equation model (PLS-SEM) as a quantitative research methodology that synthesizes factor analysis, regression analysis, and path analysis to examine multifactorial causal relationships in complex systems [25]. Compared with traditional analytical methods, this method can better distinguish the direct, indirect and overall effects among factors. Therefore, the PLS-SEM was used to analyze the composite factors and interactions that control wetland variation in this study. In addition, geographically weighted regression (GWR) was added to further identify localized spatial variation in the primary influences.

Wetlands in the arid and semiarid regions in northern China account for a large proportion of wetlands in China [26]. The wetland ecosystems in this region are closely related to other ecosystems and inhibit riparian deforestation, shrinking oases, grassland degradation, and desertification [27]. Compared with humid areas, wetland ecosystems in arid and semiarid areas are more vulnerable to external factors due to their more dispersed nature, small patch sizes, and relatively scarce water resources [28]. For decades, the combined effects of the human production activities and natural environment have caused wetland ecosystems in arid and semiarid areas to become sensitive and fragile, and the ecological functions and structure of these wetlands have been appreciably degraded [29]. Therefore, elucidating the spatiotemporal pattern and drivers of wetlands in this area is crucial for their conservation and restoration.

Broadly speaking, wetlands are categorized into natural and constructed wetlands; constructed wetlands are engineered systems that mimic natural wetlands [30] and are closely related to natural wetlands, but their spatiotemporal dynamics and drivers may vary. Previous studies have lacked comparative assessments of natural and constructed wetland drivers, especially in large-scale arid and semiarid regions. Therefore, the primary objectives of the study are as follows: (1) to compare the spatiotemporal dynamics and evolution directions of natural and constructed wetland areas; (2) to quantitatively compare

the direct and indirect effects of natural factors and anthropogenic interference on the changes in natural and constructed wetlands; (3) to explore the spatial heterogeneity of factors influencing the distribution of natural and constructed wetlands. The research results contribute to the scientific basis for the conservation and management of wetlands or oases in arid and semiarid areas.

2. Materials and Methods

2.1. Study Area

The arid and semiarid regions of northern China between $32^{\circ}43' N$ – $50^{\circ}12' N$ and $73^{\circ}30' E$ – $121^{\circ}51' E$ have a total area of approximately $3,362,429 \text{ km}^2$ and include seven provinces (Inner Mongolia, Hebei, Shanxi, Gansu, Qinghai, Ningxia, Xinjiang) (Figure 1). In these regions, the landform is complex and changeable, and the topography is undulating and changing, mainly composed of plateaus, mountains, and basins. The overall altitude is high, with an average of 2077 m, but there are obvious differences within the regions. The inland arid and semiarid areas have fewer sources of water vapor, and the climate is very dry [31], while the eastern fringes of arid and semiarid regions are affected by southwesterly and southeasterly monsoons. Overall, the climate types of the area mainly consist of a temperate continental climate and plateau mountain climate. The average annual rainfall is less than 400 mm, and the spatiotemporal distribution is inconsistent and varies regionally and temporally. The evaporation rate is high, and the area is prone to drought. Most of the study area lies in the inland area, with short rivers, flatland runoff, mainly from temporary water flow formed by heavy rainfall, mountain runoff, mainly recharged by rain and ice melt water, and many lakes, which are predominantly saltwater lakes. The area has low vegetation coverage, severe desertification, and a fragile ecological environment that is affected by terrain and climate [32]. Grassland and desert are the dominant land-cover types [33], and saline–alkali soil is the main soil type.

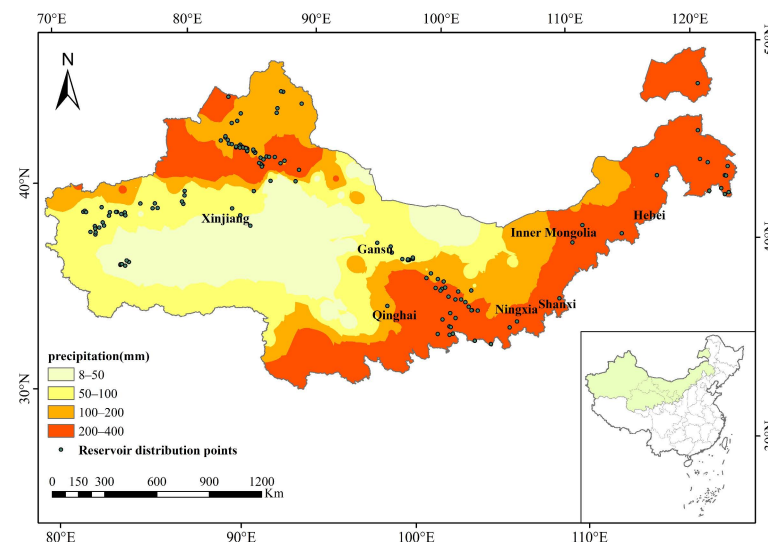


Figure 1. Locations of the arid and semiarid regions of northern China and reservoirs.

2.2. Data Sources

The datasets applied in the research include land-use, terrain, soil, moisture, heat, biology, and human-disturbance data. Land-use data were obtained from the European Space Agency (ESA) and include 6 land-use types: agriculture, grassland, forest, wetland, settlement, and other lands (shrub, sparse vegetation, and bare land). In this study, wetlands were categorized into natural and constructed wetlands; the constructed wetlands mainly comprised medium and large reservoirs due to the extensive range of the study region and the application of land-use data at a resolution of 300 m. The distribution locations of reservoirs are shown in Figure 1. A total of 149 reservoirs were searched from the

China Statistical Yearbook and Google Earth images. Natural wetlands are defined as all wetland types except constructed wetlands. The terrain data, including the elevation and slope, were generated from the Resource and Environment Science and Data Center, China (RESDC), at a resolution of 1 km. The soil data, including the percentage of clay and silt, organic carbon (OC), and pH, were collected from the Harmonized World Soil Database (HWSD) v1.2. Soil moisture (SM) was obtained from the ESA. Moisture data containing precipitation and wet day frequency (WDF) were collected from the Climatic Research Unit (CRU), and runoff data were obtained from the Institute of Tibetan Plateau Research (TPDC). Heat data, including temperature and evaporation, were obtained from CRU. Biological data, consisting of the leaf area index (LAI) and normalized difference vegetation index (NDVI), were collected from the RESDC. Human-disturbance data, including GDP and population from the RESDC, arable land area, and urban area, were calculated from the land-use data of the ESA, and water consumption data were collected from the Ministry of Water Resources of China (MWR). In this research, except for the land-use data, the rest of the data were reinterpolated to a resolution of 1 km. Detailed information on all data are presented in Table 1.

Table 1. Data sources.

Category	Data	Resolution	Year	Data Resource	
Wetland	Wetland area (km ²)	300 m	1995–2019	ESA_LUCC (https://www.esa-landcover-cci.org/ , accessed on 14 March 2022)	
Terrain	Elevation (m)	1 km	2000	RESDC (http://www.resdc.cn/ , accessed on 22 May 2022)	
	Slope (°)	1 km			
Soil	Clay (%)	1 km	2008	HWSD v1.2 (http://www.fao.org/ , accessed on 7 July 2022)	
	Silt (%)	1 km			
	pH	1 km			
	OC(%)	1 km			
Moisture	SM(m ³ /m ³)	25 km	1995–2019	ESA_CCI_SM (http://www.esa-soilmoisture-cci.org , accessed on 8 July 2022)	
	Precipitation (mm)	50 km	1995–2019	CRU (https://data.ceda.ac.uk/badc/cru/data/cru_ts/cru_ts_4.05/ , accessed on 10 July 2022)	
	WDF(day)	50 km		TPDC (https://data.tpdc.ac.cn/ , accessed on 12 July 2022)	
Heat	Runoff(m ³ /s)	25 km	1995–2018		
	Temperature (°C)	50 km	1995–2019	CRU (https://data.ceda.ac.uk/badc/cru/data/cru_ts/cru_ts_4.05/ , accessed on 12 July 2022)	
Evaporation (mm)	50 km				
Biology	NDVI	1 km	1998–2019	RESDC (http://www.resdc.cn/ , accessed on 20 July 2022)	
	LAI	1 km	1995–2019		
Human Dis- turbance	GDP (ten thousand yuan/km ²)	1 km	1995–2019	RESDC (http://www.resdc.cn/ , accessed on 22 July 2022)	
	Population (person/km ²)	1 km			
	Arable land area (km ²)	300 m			ESA_LUCC (https://www.esa-landcover-cci.org/ , accessed on 14 March 2022)
	Urban area(km ²)	300 m			
	Water consumption(m ³)		2000–2019	MWR (http://www.mwr.gov.cn/ , accessed on 28 July 2022)	

2.3. Data Processing

To extract data on wetlands and related driving factors, a grid method was adopted. According to the area thresholds of natural and constructed wetlands in the study area, cell grids of 5 km × 5 km (natural wetlands) and 1 km × 1 km (constructed wetlands) were generated in ArcGIS 10.2, and the wetland area, arable-land area, and urban area in each grid were extracted separately. In the meantime, the average values of other driving factor data in each grid were calculated. All the resulting datasets of dependent and independent variables in each grid were used to construct the PLS-SEM model.

2.4. Methods

In this study, natural and constructed wetlands were extracted via land-use data. Next, ArcGIS 10.2 software first mapped the wetland distribution, then was combined with the land-use transfer matrix method to quantitatively analyze the spatial and temporal changes in the wetlands. In addition, SmartPLS 3.3.3 software was combined with wetland data and driving factor data to build the PLS-SEM of natural and constructed wetlands, which was used to systematically analyze the driving mechanism of wetlands. Finally, the GWR model was employed to discuss the spatial nonstationarity of the driving factors of natural and constructed wetlands. The detailed flow chart is presented in Figure 2.

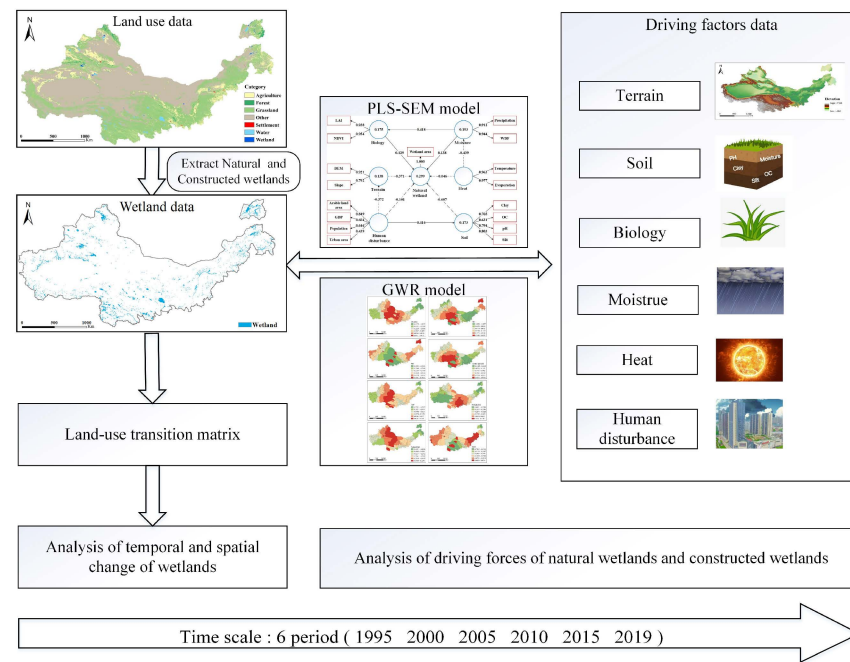


Figure 2. Flowchart of the study.

2.4.1. Land-Use Transfer Matrix and Dynamic Index

The land-use transfer matrix applies Markov models to land-use changes. It can clearly reflect the transfer and change characteristics between divergent wetland types and between wetlands and other land-use types in a specific period. The calculation formula is expressed as follows [34]:

$$X = \begin{bmatrix} X_{11} & X_{12} & \cdots & X_{1j} \\ X_{21} & X_{21} & \cdots & X_{2j} \\ \vdots & \vdots & \ddots & \vdots \\ X_{i1} & X_{i2} & \cdots & X_{ij} \end{bmatrix} \tag{1}$$

where X_{ij} means the area transferred from land-use type i to j .

The calculation formula of the land-use type dynamic index is as follows [35]:

$$K = \frac{U_b - U_a}{U_a} \times \frac{1}{T} \times 100\% \tag{2}$$

where K represents the annual rate of change in a certain type of land-use during the study period. U_a and U_b are the areas of a single land-use type at the start and end of the research, respectively. T is the study period, and the unit is years.

2.4.2. PLS-SEM

The PLS-SEM is a structural equation model based on the partial least-squares method and is used to assess causal effects between latent variables of construction. It typically

consists of measurement and structural model. The partial least-squares algorithm can handle the multicollinearity problem better than the traditional principal component analysis, ridge regression and least-squares method, which is helpful to achieve the research purpose of this paper [36].

There are two types of variables in the PLS-SEM; namely, observed variables that can be measured directly and latent variables. The measurement model joins the observed variable (x_{jh}) to its corresponding latent variable, also known as the external model. The specific algorithm is as follows [37]:

$$X_{jh} = \lambda_{jh}\zeta_{jh} + \varepsilon_{jh} \quad (3)$$

where λ_{jh} denotes the coefficient of the column vector (ζ_j) and ε_{jh} denotes the random error.

The structure model describes the causal relationship between different latent variables, normally expressed by a linear equation [38]:

$$\zeta_j = \sum_{i \neq j} \beta_{ij}\zeta_i + \zeta_j \quad (4)$$

where β_{ij} is the path coefficient among the latent variables. ζ_j is the stochastic error term that meets the forecast-specified condition in the above equation; that is, the residual average value is 0, which is unrelated to ζ_j .

The PLS-SEM evaluation mainly tests for reliability and validity. Composite reliability (CR) and Cronbach's alpha are commonly used to verify the reliability of internal consistency. Generally, Cronbach's alpha and CR values above or equal to 0.6 are acceptable, but if above or equal to 0.7, the calculated results are satisfactory. The measure used to evaluate the convergence effectiveness of a structure is the average variance extraction (AVE) of all terms on each structure [39], and an AVE typically needs to be greater than 0.5; rho_A is also an indicator for model validation, and its value must be greater than 0.7.

2.4.3. GWR Model

The GWR model as a reformulation of traditional linear regression that addresses spatial heterogeneity using local smoothing [40]; it effectively reveals the spatial nonstationarity of the relationship among variables. In this study, GWR was applied to quantify the spatial heterogeneity between wetlands and the driving factors. The expression for the GWR model is as follows [41]:

$$y_i = \beta_0(u_i, v_i) + \sum_{j=1}^k \beta_j(u_i, v_i)x_{ij} + \varepsilon_i \quad (5)$$

where y_i represents a dependent variable denoting the wetland area in the i th unit, x_{ij} represents the j th independent variable at location (u_i, v_i) , which is the driving factor, $\beta_j(u_i, v_i)$ is the intercept at position (u_i, v_i) , k is the sum of the factors, while ε_i represents the random error term.

3. Results

3.1. Spatiotemporal Variations in the Wetland Area in Arid and Semiarid Regions of Northern China

From 1995 to 2019, the area of wetlands showed an overall upward trend (Figure 3). Natural wetlands continued to rise, except for a slight decline in 2000, increasing by 1423.71 km² by the end of 2019, with a change rate of 4.16% and an annual change rate (K) of 0.17%. The period with the largest rate of change was from 2015 to 2019, at 1.44% and with a K of 0.29% (Table 2). Although constructed wetlands increased by only 191.61 km² from 1995 to 2019, their overall growth rate of 11.86% was much higher than that of natural wetlands. Since 2000, the rates of change in constructed wetlands have continued to

decrease. From 2015 to 2019, the rate of change was the lowest, at 0.26%, and the K was only 0.05% (Table 3).

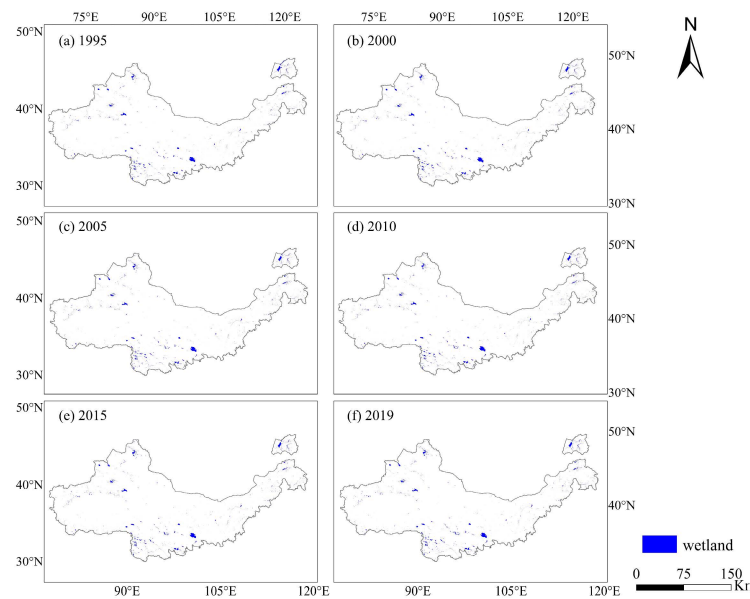


Figure 3. Spatial patterns of wetlands in the study area.

Table 2. Changes in the area of natural wetlands during different stages from 1995 to 2019.

Year	Wetland(km ²)	Stage	Change Area (km ²)	Change Rate (%)	K (%)
1995	34,243.92	1995–2000	−93.78	−0.27%	−0.05%
2000	34,150.14	2000–2005	322.11	0.94%	0.19%
2005	34,472.25	2005–2010	464.22	1.35%	0.27%
2010	34,936.47	2010–2015	226.35	0.65%	0.13%
2015	35,162.82	2015–2019	504.81	1.44%	0.29%
2019	35,667.63	1995–2019	1423.71	4.16%	0.17%

Table 3. Changes in the area of constructed wetlands during different stages from 1995 to 2019.

Year	Wetland (km ²)	Stage	Change Area (km ²)	Change Rate (%)	K (%)
1995	1614.96	1995–2000	18.45	1.14%	0.23%
2000	1633.41	2000–2005	65.43	4.01%	0.80%
2005	1698.84	2005–2010	59.49	3.50%	0.70%
2010	1758.33	2010–2015	43.47	2.47%	0.49%
2015	1801.80	2015–2019	4.77	0.26%	0.05%
2019	1806.57	1995–2019	191.61	11.86%	0.49%

Concerning spatial pattern changes from 1995 to 2019, the stable and unchanging areas of natural and constructed wetlands were widely distributed at 30,661.11 km² and 1291.50 km², accounting for 78.12% and 60.63% of their total area, respectively. In addition, the reduced natural wetland area was small, at 3782.81 km², accounting for only 9.13%, with a scattered distribution. The reduced area of the constructed wetland was 323.46 km² or 15.19% of the overall area, and was primarily distributed as small patches in the margins of reservoirs. The natural wetland area increased to 5006.52 km², accounting for 12.76% of the total area; it was primarily centered in the central and northwestern parts of the study region. The increased area of constructed wetlands was dispersed and increased to 515.07 km², accounting for 24.18% of the overall area (Figures 3 and 4).

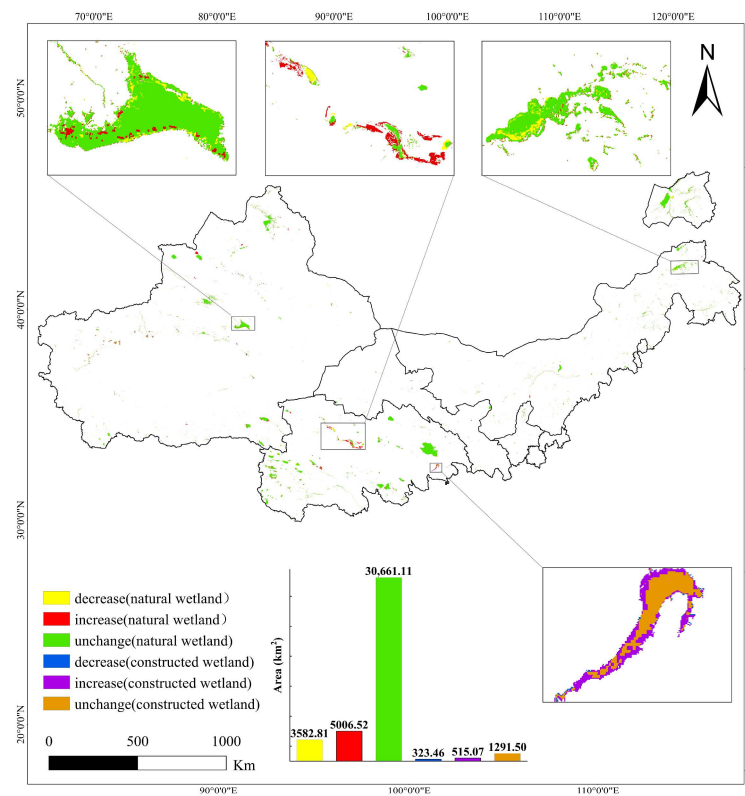


Figure 4. The spatial distribution map of natural and constructed wetland dynamics from 1995 to 2019.

3.2. Evolution of Wetland Areas in Arid and Semiarid Regions of Northern China

From 1995 to 2019, the increased area of natural wetland mainly resulted from the transformation of grassland and other lands, with net increases of 669.60 km² and 858.06 km², respectively. The decrease in natural wetland area was primarily due to transformation into agricultural land, with a corresponding net decrease area and rate of 151.38 km² and −10.63%, respectively (Table 4). During this time period, the increased area of constructed wetlands was largely caused by the transformation of grassland and other lands, among which grassland was the greatest, with a net transformed area of 138.33 km², almost twice that of other lands. In addition, the conversion of constructed wetlands to other lands was relatively small; the net conversion rate of agricultural land, which saw the most conversion, was only 3.19% (Table 4). The amount of conversion between natural wetlands and constructed wetlands was also very small. Only 8.28 km² of natural wetlands were transferred to constructed wetlands, and only 21.24 km² of constructed wetlands were converted to natural wetlands (Table 4).

Table 4. Conversion matrix of land use area from 1995 to 2019.

	1995	Natural Wetland	Constructed Wetland	Agriculture	Forest	Grassland	Settlement	Others
2019	natural wetland	29,177.10	21.24	984.06	98.55	2876.13	2.61	2460.6
constructed wetland	8.28	1407.42	57.24	1.17	210.60	0.00	121.32	
agriculture	1135.44	63.36	208,669.3	1262.61	58,546.26	54.27	31,838.85	
forest	57.42	1.53	1600.65	20,894.13	8103.96	0.09	257.49	
grassland	2206.53	72.27	56,454.03	5540.31	1,028,456.28	37.89	127,577.88	
settlement	40.77	2.07	2535.12	8.82	3014.46	1179.27	977.13	
others	1602.54	48.87	9731.25	397.53	97,664.58	19.35	1,653,423.66	

3.3. Driving Forces of Wetland Distribution Based on PLS-SEM

3.3.1. PLS-SEM Evaluation

The correlation reliability and validity test indicators Cronbach's alpha, rho_A, and CR of the PLS-SEM for natural and constructed wetlands were all above 0.7, and the AVE values were all greater than 0.5 (Tables 5 and 6), which were all within the acceptable range, proving that the model achieved good results and had certain reliability and applicability. The p values for both the external and internal loads of the model were less than 0.05, and were significant. The β values of biology, human disturbance, terrain, soil, moisture, and heat factors and its interactive effects were also found to be statistically significant. In conclusion, the aforementioned indicators basically met the ideal criteria, demonstrating the reasonability and dependability of the evaluation model.

Table 5. Reliability and validity evaluation of the PLS-SEM of natural wetlands.

Latent Variables	Cronbach's Alpha	rho_A	Composite Reliability (CR)	Average Variance Extracted (AVE)
biology	0.884	0.893	0.945	0.896
human disturbance	0.765	0.969	0.756	0.525
terrain	0.712	0.749	0.848	0.738
soil	0.745	0.757	0.837	0.565
moisture	0.725	0.765	0.846	0.650
heat	0.938	0.943	0.970	0.942

Table 6. Reliability and validity evaluation of the PLS-SEM of constructed wetlands.

Latent Variables	Cronbach's Alpha	rho_A	Composite Reliability (CR)	Average Variance Extracted (AVE)
biology	0.809	1.148	0.903	0.824
human disturbance	0.718	0.745	0.721	0.502
terrain	0.700	0.815	0.824	0.705
soil	0.701	0.762	0.786	0.509
moisture	0.914	0.922	0.946	0.854
heat	0.958	0.958	0.979	0.960

3.3.2. Driving Forces of Natural Wetlands

The standardized coefficients for all latent and observed variables affecting the distribution of natural wetlands from 1995 to 2019 can be directly found in the PLS-SEM (Figure 5). Soil, terrain, human disturbance, and heat were negatively correlated with natural wetlands. Soil had the biggest negative impact, with a path coefficient of -0.610 , followed by terrain with a path coefficient of -0.417 , which became the second largest driving force affecting the natural wetland distribution. The path coefficient for human disturbance was -0.100 , and heat had no significant influence on natural wetlands because the path coefficient was less than 0.1. It is worth noting that moisture and biology had positive impacts on natural wetlands at path coefficients of 0.165 and 0.124, respectively.

Four indirect paths linked the distribution of natural wetlands. First, two indirect paths were created by human disturbance: one was a positive indirect path with an effect of 0.154 through a negative impact on terrain (-0.369), and the other was a negative indirect path with an effect of -0.252 through a positive impact on soil (0.413). Second, the indirect pathway of moisture to natural wetlands was positive because it had a positive effect on biology (0.309). Finally, the indirect effect of heat on natural wetlands through negative effects on moisture was negative.

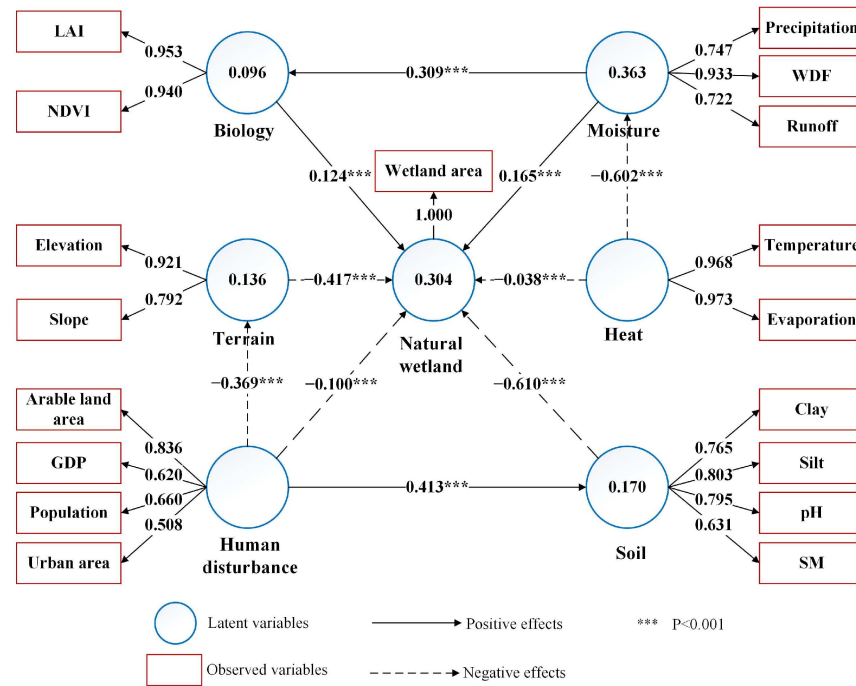


Figure 5. PLS-SEM diagram of the comprehensive influence of each variable on the change in natural wetlands.

3.3.3. Driving Forces of Constructed Wetlands

The PLS-SEM contained 7 latent variables and 17 observed variables, of which there were a total of 6 direct paths (Figure 6). The results showed that the factors of soil, terrain, and human disturbance had negative effects on constructed wetlands. Moreover, human disturbance was the dominant factor affecting constructed wetlands, with a path coefficient of -0.438 . Additionally, both heat and moisture had positive impacts on constructed wetlands, at path coefficients of 0.179 and 0.125 , respectively. Biology had little influence.

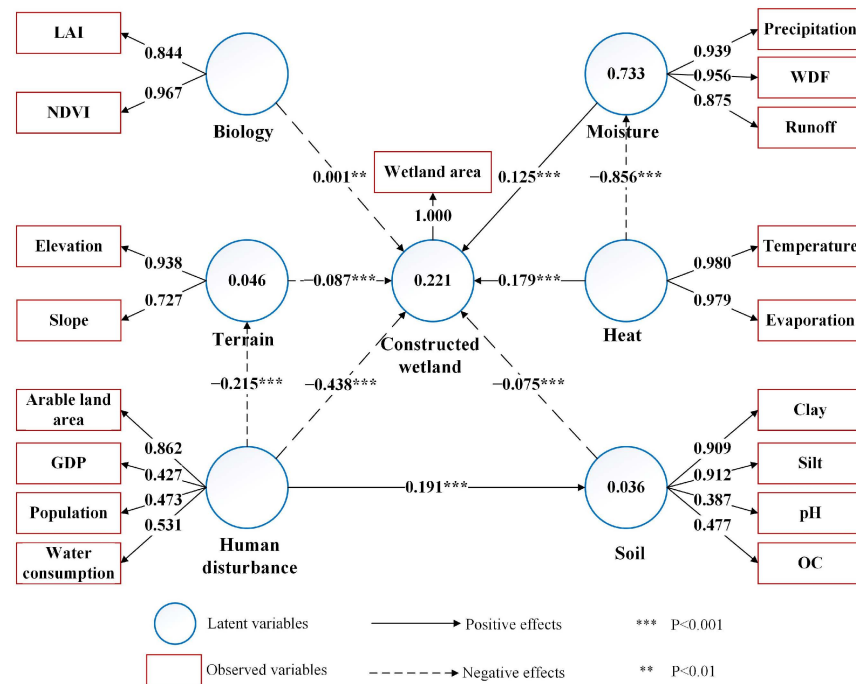


Figure 6. PLS-SEM diagram of the comprehensive influence of each variable on the change in constructed wetlands.

Three indirect paths had influence on the change in constructed wetlands. Human disturbance indirectly and positively impacted the constructed wetlands through its negative effect on terrain (-0.215). On the other hand, human disturbance had an indirect negative impact on the change in constructed wetlands via a positive impact on soil (0.191). In addition, heat had a strong negative impact on moisture (-0.856), which led to the strongest indirect negative path for constructed wetlands.

3.4. Influential Factors of Wetland Distribution

Based on the PLS-SEM results of natural wetlands and constructed wetlands, eight main indicators of elevation, slit, pH, arable land area, GDP, precipitation, temperature, and NDVI were selected for the county-scale GWR analysis (Figures 7 and 8).

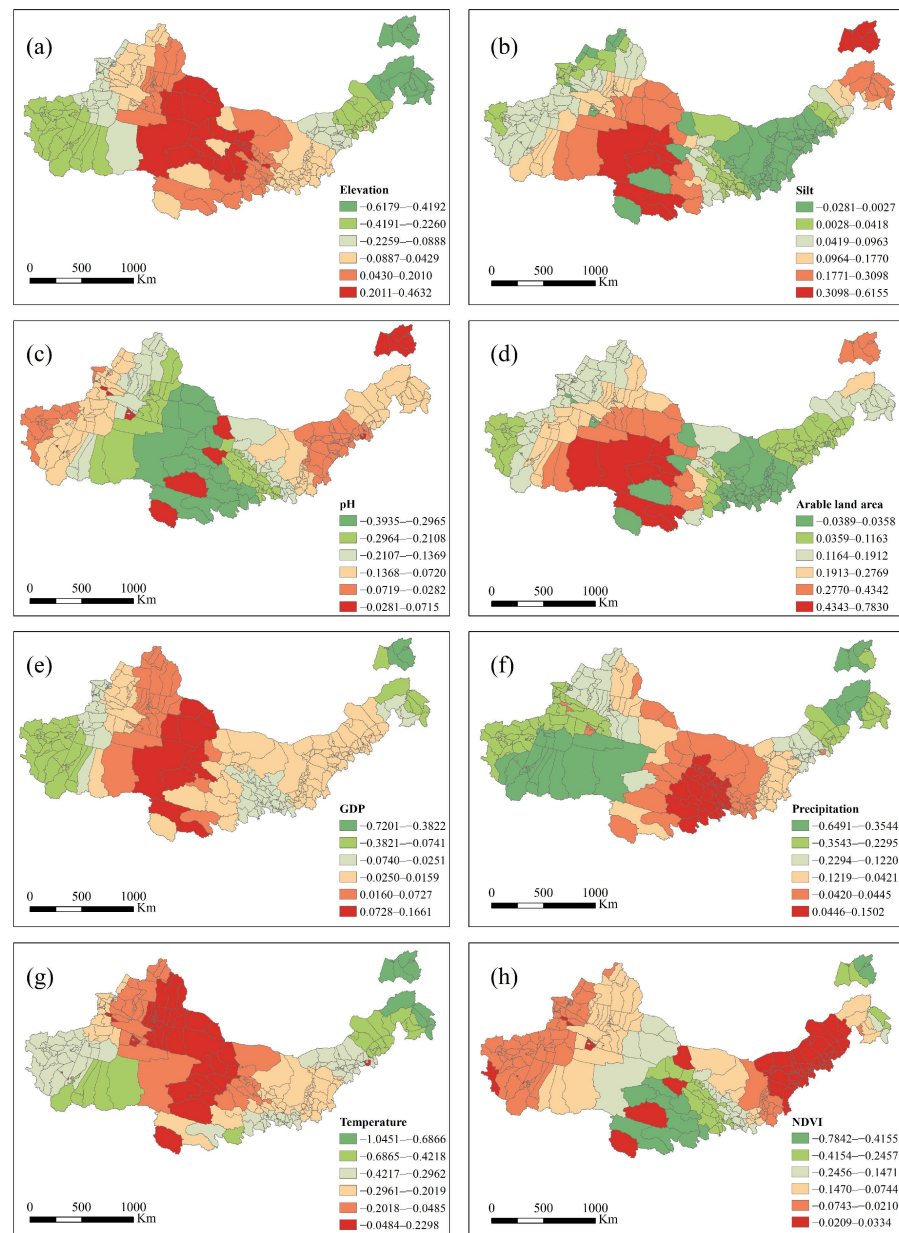


Figure 7. Regression coefficients of the spatial distribution of the main drivers of natural wetlands based on GWR. Input factor scores: (a) Elevation; (b) Silt; (c) pH; (d) Arable-land area; (e) GDP; (f) Precipitation; (g) Temperature; (h) NDVI.

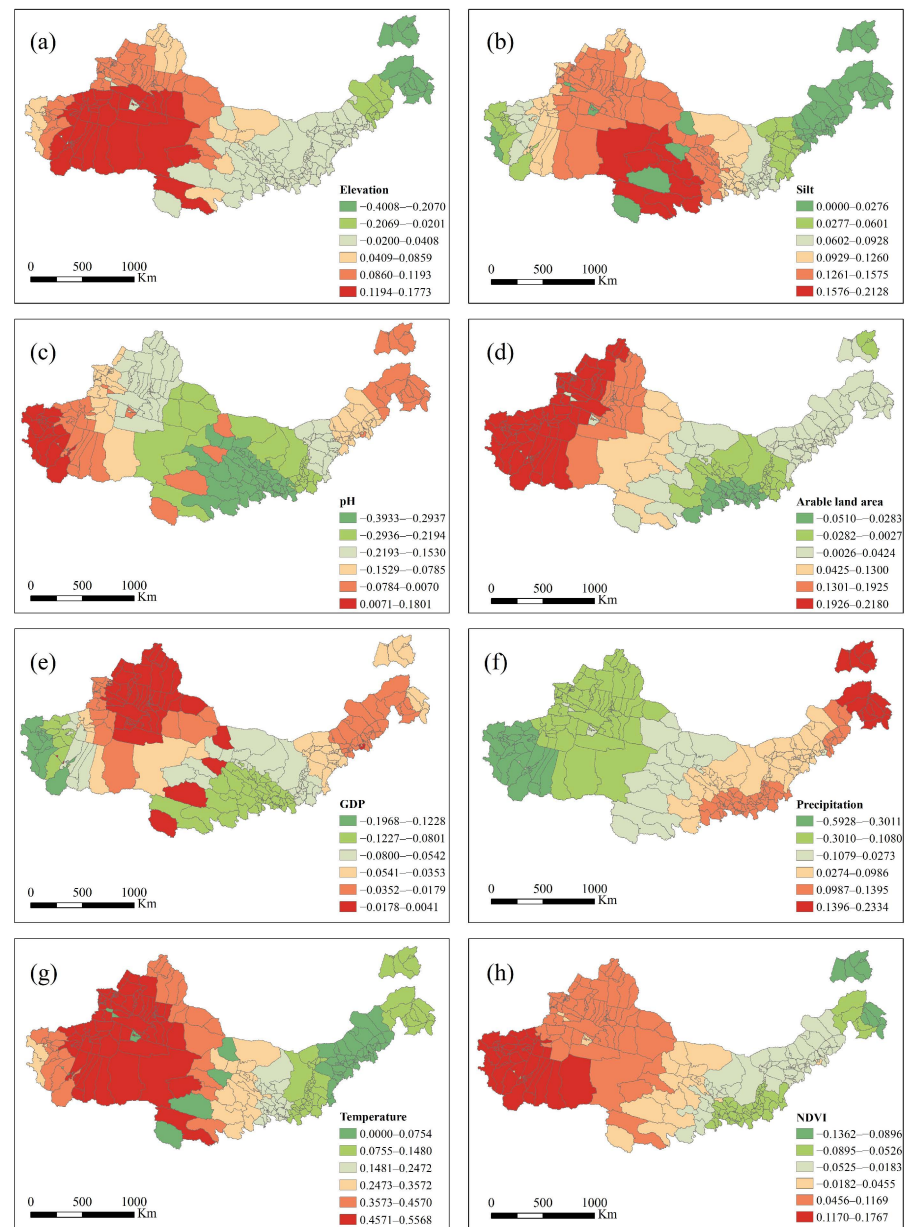


Figure 8. Regression coefficients of the spatial distribution of the main drivers of constructed wetlands based on GWR. Input factor scores: (a) Elevation; (b) Silt; (c) pH; (d) Arable-land area; (e) GDP; (f) Precipitation; (g) Temperature; (h) NDVI.

3.4.1. Spatial Heterogeneity of Driving Factors of Natural Wetlands

The regression coefficient of elevation ranged from -0.6179 to 0.4632 , showing a significant negative impact in western Xinjiang and central and eastern Inner Mongolia, and a positive effect in western Inner Mongolia, Gansu, Qinghai, Ningxia, and eastern Xinjiang (Figure 7a). The regression coefficient of silt ranged from -0.0281 to 0.6155 , with an overall positive effect, and the largest positive effect in northeastern Inner Mongolia, western Qinghai, and eastern Xinjiang (Figure 7b). The regression coefficient of pH was between -0.3935 and 0.0715 , showing a generally negative effect (Figure 7c). The regression coefficient of the arable land area ranged from -0.0389 to 0.7830 , with a mainly positive effect on wetlands, and the largest regression coefficient in eastern Xinjiang and western Qinghai (Figure 7d). The regression coefficient of GDP was from -0.7201 to 0.1661 , with a negative effect that gradually increased from the middle to the periphery (Figure 7e). The precipitation regression coefficient ranged from -0.6491 to 0.1502 ; only western Gansu and eastern

Qinghai were positively correlated, and the remaining area was negatively correlated (Figure 7f). The regression coefficient range of temperature was from -1.0451 to 0.2298 ; eastern Xinjiang, western Gansu, and western Qinghai showed positive correlations, while the remaining areas demonstrated negative correlations (Figure 7g). The regression coefficient of the NDVI ranged from -0.7842 to 0.0334 , and its overall performance was negatively correlated (Figure 7h).

3.4.2. Spatial Heterogeneity of Driving Factors of Constructed Wetlands

The regression coefficient of elevation was from -0.4008 to -0.1773 , and the impact on constructed wetlands gradually changed from positive in the west to negative in the east (Figure 8a). The regression coefficient of silt was between 0.0000 and 0.2128 , and all regions had an overall positive impact, with the largest effects in southeastern Xinjiang and central Qinghai (Figure 8b). The regression coefficient of pH was from -0.3933 to 0.1801 , except for western Xinjiang, which showed a positive correlation, and all other regions were negatively correlated (Figure 8c). The regression coefficient of the arable land area was between -0.0510 and 0.2180 , with the largest positive impact in Xinjiang and the largest negative impact in eastern Qinghai and southern Gansu (Figure 8d). The regression coefficient of GDP was from -0.1968 to 0.0041 , the overall impact on wetlands was negative, and the largest negative correlation was in western Xinjiang (Figure 8e). The regression coefficients of precipitation were between -0.5928 and 0.2334 , and the impact on constructed wetlands gradually shifted from negative in the west to positive in the east (Figure 8f). The regression coefficient of temperature was from 0.0000 to 0.5568 , with an overall positive correlation, and the maximum correlation was reached in Xinjiang and western Qinghai (Figure 8g). The distribution of regression coefficients of NDVI indicated positive effects in Xinjiang, western Qinghai, western Gansu, and northwestern Inner Mongolia, and negative effects in the remaining areas (Figure 8h).

4. Discussion

4.1. Spatiotemporal Changes in Wetlands

From 1995 to 2019, overall, wetland area in the arid and semiarid regions of northern China presented an increasing trend, and the a growth rate of 4.5% (Figure 3). The overall growth rate of natural wetlands was 4.16% (Table 2). This growth may be due to the implementation of a number of ecological conservation and restoration initiatives. Starting in 2000, the Chinese government started to substantially invest in the conservation and restoration of natural capital; the National Action Plan for Wetland Conservation was also developed in that year [42]. The National Wetland Conservation Engineering Plan (NWCEP) 2002–2030 was approved in 2003 [43]. The area of constructed wetlands continued to rise, with an overall growth rate of 11.86%, much higher than that of natural wetlands (Table 3). This positive result is mainly due to the implementation of water resource engineering [44,45]. However, it is important to note that, from 2000 onward, the growth rate of artificial wetlands continued to decline (Table 3). This decline may be attributed to the increased focus on water conservation and ecological construction in modern water projects, and rather than a single-minded exploitation, the focus has shifted to management and sustainability [46]. In addition, it can be observed from the land-use transfer matrix that other lands have had the highest contribution rate to the increase in natural wetland area, while the proportion of bare land in other lands was as high as 86.88%, which reflects the long-term commitment of the Chinese government to desertification control in arid and semiarid areas; these actions have achieved certain results over the years [47]. Moreover, grassland had the greatest contribution to the increase in constructed wetlands, suggesting that the expansion of reservoir areas drives land-use type transitions. Water expansion inevitably led to an increase in land-cover types, such as grassland, which developed directly by these water bodies.

4.2. Driving Forces of Wetland Change

4.2.1. Direct Effects on Wetland Distribution

A comparison of the PLS-SEM of natural and constructed wetlands (Figures 5 and 6) shows that the main driver of natural wetlands was clearly natural factors, but the main driver of constructed wetlands was human factors.

Soil played a dominant role in the distribution of natural wetlands, indicating that soil salinization and texture changes severely disturbed the ecological environment of natural wetlands in arid and semiarid areas [48] by impacting soil nutrient loss, biological community composition changes, and biological reduction; these impacts led to a strong negative effect relationship between the soil and natural wetlands [49]. Compared with natural wetlands, soil has a less negative impact on constructed wetlands, possibly because reservoir seepage raises the groundwater table downstream, which exacerbates soil salinization in natural wetlands downstream of reservoirs [50]. In addition, GWR showed that soil responded to natural wetlands more than constructed wetlands, though these effects were localized in space. The central counties were the most sensitive in response, a finding that may be due to higher population pressure in the middle of the study area, which triggered anthropogenic soil erosion and land depletion [51].

The influence of human disturbance on wetlands is extraordinarily complicated. This study showed that human disturbance was the dominant driving factor for the change in constructed wetlands. With increased human activities, population growth, faster economic development, and greater water demand, the water supply inevitably increases, and the water area of constructed wetlands decreases [52]. Therefore, a strong negative correlation exists between human disturbance and constructed wetland distribution. Contrary to the driving mechanism of constructed wetlands, human disturbance had a weaker impact on natural wetlands. However, previous research has demonstrated that human activity is the major contributor to wetland loss [53–56]. This difference is because human beings have not yet strongly exploited natural wetlands in arid and semiarid regions [57]. Furthermore, natural wetlands were less likely than other regions to be converted into farmland and construction land. Although the influence of human disturbances on natural wetlands was not significant, it should not be ignored. According to the GWR results (Figures 7 and 8), different regions have different degrees of response to human disturbance. However, compared to other regions, the vast majority of wetlands in Xinjiang are less affected by human disturbance and even experience positive impacts. This may be attributed to the effective implementation of wetland protection policies in Xinjiang, which have been used through Xinjiang to prevent damage from human activities; one example is the construction of fencing to provide a solid protective barrier for wetlands [58].

In terms of terrain driving forces, some studies have demonstrated that flat and low-lying terrain conditions are more conducive than other terrains to natural wetland formation and development because these areas receive more water input from highlands during snowmelt runoff or landfill overflow events in spring [59,60]. Therefore, terrain elevation and slope are negatively correlated with wetlands. Notably, terrain has less influence on constructed wetlands. The elevation and slope of the constructed wetlands did not change greatly over time and have been more stable than the terrain of natural wetlands. In addition, the natural wetland in the GWR model was more sensitive to elevation than the constructed wetland, proving this point (Figures 7a and 8a). However, it is worth noting that the wetlands in the northern part of the Tibetan Plateau were less sensitive to elevation because, although the region is characterized by high elevation, the overall internal terrain is relatively flat, and most of the wetlands are distributed in the basins and depressions of the plateau region [61].

The results of this study indicated that the higher the temperature and evaporation, the faster the wetland shrinks, which is consistent with [62], who show that high temperature increases the rate of evaporation of wetland surface water and changes the wetland water cycle; thus, many extreme weather events caused by global warming may pose a risk to wetlands. Temperature and potential evapotranspiration have been increasing in the

arid and semiarid regions of northern China for several decades, with more significant changes in the eastern and western parts of the study area, which indicates that these areas are significantly more sensitive to natural wetland response than those in the central part of the region (Figure 7g) [63]. However, unlike natural wetlands, constructed wetlands showed a positive correlation with heat in this study, which was consistent with the findings of the national wetland resources survey in China concerning the relationship between reservoir wetland area change and air temperature [64]; this result was confirmed by the positive response of the constructed wetlands to temperature in each region of the GWR (Figure 8g). Additionally, precipitation has a positive effect on wetlands, potentially because precipitation affects the groundwater table in wetlands and provides recharge water [65]. Moreover, precipitation is the major driver of river runoff. The more precipitation there is, the greater the inflow of the reservoir [66]. Biological factors have little effect on both natural and constructed wetlands. Some studies have revealed that the health of wetlands is rarely correlated with aboveground biomass [67–69]. Perhaps more attention should be given to underground biomass, but the characteristics of underground biomass cannot be directly correlated with the surface reflectance from remote sensing [70]. Therefore, in addition to remote sensing products such as NDVI and LAI, other indicators that can better reflect underground biomass deserve further exploration.

4.2.2. Indirect Effects on Wetland Distribution

The PLS-SEM suggested that driving factors not only directly affect wetland distribution, but some factors even have opposite effects through indirect pathways, thus sufficiently illustrating the complexity of the driving mechanism of wetlands.

This study showed that human disturbance accelerated the direct negative effect of soil on wetland distribution through its positive influence on soil (Figures 5 and 6). Human-related activities, for example urbanization building and land reclamation, lead to an increase in clay and silt in soil [71], which then destroys the soil environment suitable for wetland development. On the other hand, human disturbance positively impacts wetlands through negative effects on terrain. Human activities have been recognized as a significant geomorphic factor, and the resulting changes in land cover and geomorphology are global issues [72]. For instance, the activities of agriculture, mining, quarrying, road building, etc., cause surface changes, resulting in changes in the elevation and slope of terrain in some areas, thus affecting wetland distribution [73].

The results of the study also found that heat had an indirect negative impact on wetlands through a pronounced negative effect on moisture (Figures 5 and 6). Previous studies have also revealed that global-warming-induced increases in evaporation and decreases in precipitation can destroy the wetland hydrological environment [74]. Water is a key factor limiting plant growth in arid and semiarid regions [75]. Adequate water replenishment maintains the wetland water level and affects wetland plant growth [76]. Hence, water indirectly improves the living environment of natural wetlands through its positive effects on plants, which ultimately influences the distribution of natural wetlands. In contrast, plants in constructed wetlands are not indirectly influenced by global-warming-induced hydrological changes (Figure 6).

4.3. Implications for Wetland Management

Despite increases in global wetland degradation [77], wetlands in the arid and semiarid regions of northern China showed an increasing trend, which means that wetland conservation in the region have achieved some success. Some important directions for future wetland conservation in the region are indicated in this study. First, the PLS-SEM showed that soil was the most important driving force of natural wetlands, implying that the influence of soil factors should be given priority in the management of natural wetlands. Corresponding soil protection and control measures can be taken, such as controlling soil salinization, sanding and barrenness caused by overcultivation and overgrazing [78], and mitigating the impact of artificial activities on soil quality. Furthermore, human disturbance

caused the greatest negative effect on constructed wetlands. Thus, water extraction should be strictly controlled to ensure that the ecological water needs of reservoirs in arid and semiarid regions is met. In addition, ecological impacts should be taken seriously during hydraulic project construction, with the harmony of people and water being a top priority. In addition, long-term drought monitoring is necessary to prevent the adverse effects of drought on wetlands [79]. More importantly, this study can help wetland ecosystem managers further understand the adverse effects of the interactions among various influencing factors on wetlands, such as human activities that can affect wetlands by modulating terrain and soil. Moreover, the GWR visualized the spatial-scale responses of various driving forces to county-level wetlands. For counties with a high sensitivity in the study area, GWR can be targeted to provide credible guidance to regional wetland managers. Especially for areas rich in agricultural production activities and that experience significant climate change, the government should further increase the protection of wetlands. However, due to the limitation of data sources, there is room for further improvement to indicator system of drivers of wetland evolution; for example, pollution factors and natural-disaster factors, which influence discharge into wetlands, can degrade wetland ecosystem functions [80]. In future research, various factors that effectively conserve and actively restore wetland ecosystems should be considered, thus enabling the construction of a solid ecological barrier for sustainable socioeconomic development in northern China.

5. Conclusions

This study explored the responses of wetlands to soil, terrain, human disturbance, heat, moisture, and biology, and showed that these driving factors have different interactions with different wetland types. The findings of the study indicated that, from 1995 to 2019, natural and constructed wetlands increased by 1423.71 km² and 191.61 km², respectively, and the increases in both wetland types were mainly from grasslands and other lands. Soil and terrain factors directly influenced the changes and distribution in natural wetlands, while human disturbances directly influenced the changes and distribution in constructed wetlands. In addition, the positive effect of human disturbance on soil exacerbated the negative impact of soil on wetlands; the negative effect of human disturbance on terrain weakened the negative effect of terrain on wetlands; the negative effect of heat on moisture weakened the positive effect of moisture on wetlands; the positive effect of water on biology enhanced the positive effect of biology on natural wetlands, though this effect did not extend to constructed wetlands. The combination of the PLS-SEM and GWR methods revealed the spatial heterogeneity and interaction of various driving factors in the long-term evolution of wetlands and implied the complexity of causality in controlling the distribution of wetlands; these results indicate that natural and constructed wetlands should be targeted differently with different management and conservation measures. The findings of the study are meaningful for exploring the driving mechanisms of wetlands in arid and semiarid areas, and especially for providing insights into the comparative analysis of influencing factors of different wetlands.

Author Contributions: Conceptualization, J.Z., J.C. and Y.Q.; methodology, Y.Q., Y.Z. and X.L.; software, Y.Q., Y.Z. and X.L.; data curation J.Z. and J.C.; formal analysis, Y.Q.; writing—original draft preparation, J.Z. and Y.Q.; writing—review and editing, J.Z. and J.C.; visualization, Y.Z. and X.L.; funding acquisition, J.Z. and J.C. All authors have read and agreed to the published version of the manuscript.

Funding: This research received no external funding.

Data Availability Statement: Not applicable.

Conflicts of Interest: The authors declare no conflict of interest.

References

1. Zheng, Y.; Liu, H.; Zhuo, Y.; Li, Z.; Liang, C.; Wang, L. Dynamic changes and driving factors of wetlands in Inner Mongolia Plateau, China. *PLoS ONE* **2019**, *14*, 8. [[CrossRef](#)]
2. Gunderson, L.H.; Cosens, B.; Garmestani, A.S. Adaptive governance of riverine and wetland ecosystem goods and services. *J. Environ. Manag.* **2016**, *183*, 353–360. [[CrossRef](#)] [[PubMed](#)]
3. Kingsford, R.T.; Basset, A.; Jackson, L. Wetlands: Conservation's poor cousins. *Aquat. Conserv.* **2016**, *26*, 892–916. [[CrossRef](#)]
4. Hu, S.; Niu, Z.; Chen, Y.; Li, L.; Zhang, H. Global wetlands: Potential distribution, wetland loss, and status. *Sci. Total Environ.* **2017**, *586*, 319–327. [[CrossRef](#)] [[PubMed](#)]
5. Sica, Y.V.; Quintana, R.D.; Radeloff, V.; Gavier-Pizarro, G. Wetland loss due to land use change in the Lower Paraná River Delta, Argentina. *Sci. Total Environ.* **2016**, *568*, 967–978. [[CrossRef](#)] [[PubMed](#)]
6. Davidson, N.C. How much wetland has the world lost? Long-term and recent trends in global wetland area. *Mar. Freshwater Res.* **2014**, *65*, 934–941. [[CrossRef](#)]
7. López-Merino, L.; Cortizas, A.M.; López-Sáez, J.A. Human-induced changes on wetlands: A study case from NW Iberia. *Quat. Sci. Rev.* **2011**, *30*, 2745–2754. [[CrossRef](#)]
8. Yu, H.Y.; Zhang, F.; Kung, H.T.; Johnson, V.C.; Bane, C.S.; Wang, J.; Ren, Y.; Zhang, Y. Analysis of land cover and landscape change patterns in Ebinur Lake Wetland National Nature Reserve, China from 1972 to 2013. *Wetl. Ecol. Manag.* **2017**, *25*, 619–637. [[CrossRef](#)]
9. Wang, M.J.; Qi, S.Z.; Zhang, X.X. Wetland loss and degradation in the Yellow River Delta, Shandong Province of China. *Environ. Earth Sci.* **2012**, *67*, 185–188. [[CrossRef](#)]
10. Chen, D.; Lu, X.; Hu, W.; Zhang, C.; Lin, Y. How urban sprawl influences eco-environmental quality: Empirical research in China by using the Spatial Durbin model. *Ecol. Indic.* **2021**, *131*, 108113. [[CrossRef](#)]
11. Fluet-Chouinard, E.; Stocker, B.D.; Zhang, Z.; Malhotra, A.; Melton, J.R.; Poulter, B.; Kaplan, J.O.; Goldewijk, K.K.; Siebert, S.; Minayeva, T. Extensive global wetland loss over the past three centuries. *Nature* **2023**, *614*, 281–286. [[CrossRef](#)] [[PubMed](#)]
12. Junk, W.J.; An, S.Q.; Finlayson, C.M.; Gopal, B.; Kvet, J.; Mitchell, S.A.; Mitsch, W.J.; Robarts, R.D. Current state of knowledge regarding the world's wetlands and their future under global climate change: A synthesis. *Aquat. Sci.* **2013**, *75*, 151–167. [[CrossRef](#)]
13. Wang, D.W.; Bai, J.H.; Wang, W.; Zhang, G.L.; Cui, B.S.; Liu, X.H.; Li, X.W. Comprehensive assessment of soil quality for different wetlands in a Chinese delta. *Land Degrad. Dev.* **2018**, *29*, 3783–3794. [[CrossRef](#)]
14. Kahlolo, N.; Mapeshoane, B.; Chatanga, P.; Seleteng-Kose, L.; Marake, M.V. Assessing wetland functionality using soil surface indicators in Letseng-la-Letsie wetland in Quthing District, Lesotho. *Afr. J. Range Sci.* **2021**, *38*, 110–121. [[CrossRef](#)]
15. Gao, J.; Li, X.L.; Brierley, G. Topographic influence on wetland distribution and change in Maduo County, Qinghai-Tibet Plateau, China. *J. Mt. Sci.* **2012**, *9*, 362–371. [[CrossRef](#)]
16. Kim, G.-R.; Kim, H.-R.; Choi, H.-S.; Han, J.-G.; Kim, S.-Y.; Kim, C.-S. Phylogenetic relationship of Araliaceae in Korea by seed morphological characteristics. *J. Wetl. Res.* **2015**, *17*, 139–145. [[CrossRef](#)]
17. Li, Z.; Liu, M.; Hu, Y.; Xue, Z.; Sui, J. The spatiotemporal changes of marshland and the driving forces in the Sanjiang Plain, Northeast China from 1980 to 2016. *Ecol. Process.* **2020**, *9*, 24. [[CrossRef](#)]
18. Li, S.; Dong, B.; Gao, X.; Wang, P.; Ye, X.K.; Xu, H.; Ren, C. Land use change and driving forces in Shengjin Lake wetland in Anhui province, China. *J. Appl. Remote Sens.* **2021**, *15*, 042404. [[CrossRef](#)]
19. Song, K.; Wang, Z.; Du, J.; Liu, L.; Zeng, L.; Ren, C. Wetland degradation: Its driving forces and environmental impacts in the Sanjiang Plain, China. *Environ. Manage.* **2014**, *54*, 255–271. [[CrossRef](#)]
20. Zhang, Y.; Yan, J.; Cheng, X.; He, X. Wetland Changes and Their Relation to Climate Change in the Pumqu Basin, Tibetan Plateau. *Int. J. Environ. Res. Public Health* **2021**, *18*, 2682. [[CrossRef](#)]
21. Yang, Y.; Yin, X.; Yang, Z. Environmental flow management strategies based on the integration of water quantity and quality, a case study of the Baiyangdian Wetland, China. *Ecol. Eng.* **2016**, *96*, 150–161. [[CrossRef](#)]
22. Wu, X.; Ma, T.; Wang, Y. Surface water and groundwater interactions in wetlands. *J. Earth Sci.* **2020**, *31*, 1016–1028. [[CrossRef](#)]
23. Li, Z.; Jiang, W.; Wang, W.; Chen, Z.; Ling, Z.; Lv, J. Ecological risk assessment of the wetlands in Beijing-Tianjin-Hebei urban agglomeration. *Ecol. Indic.* **2020**, *117*, 106677. [[CrossRef](#)]
24. Sarkar, S.; Parihar, S.M.; Dutta, A. Fuzzy risk assessment modelling of East Kolkata Wetland Area: A remote sensing and GIS based approach. *Environ. Model Softw.* **2016**, *75*, 105–118. [[CrossRef](#)]
25. Grace, J.B. *Structural Equation Modeling and Natural Systems*; Cambridge University Press: Cambridge, UK, 2006.
26. Jeelani, N.; Yang, W.; Xia, L.; Zhu, H.L.; An, S.Q. Ecosystem threats and management strategies for wetlands in China. *Mar. Freshwater Res.* **2020**, *71*, 1557–1563. [[CrossRef](#)]
27. Liu, B.; Zhao, W.Z.; Wen, Z.J.; Zhang, Z.H. Response of water and energy exchange to the environmental variable in a desert-oasis wetland of Northwest China. *Hydrol. Process.* **2014**, *28*, 6098–6112. [[CrossRef](#)]
28. Wang, Z.C.; Zhao, H.Y.; Zhao, C.L. Temporal and Spatial Evolution Characteristics of Land Use and Landscape Pattern in Key Wetland Areas of the West Liao River Basin, Northeast China. *J. Environ. Eng. Landsc.* **2022**, *30*, 195–205. [[CrossRef](#)]
29. Jiang, P.H.; Cheng, L.; Li, M.C.; Zhao, R.F.; Huang, Q.H. Analysis of landscape fragmentation processes and driving forces in wetlands in arid areas: A case study of the middle reaches of the Heihe River, China. *Ecol. Indic.* **2014**, *46*, 240–252. [[CrossRef](#)]

30. Ghermandi, A.; Van Den Bergh, J.C.; Brander, L.M.; De Groot, H.L.; Nunes, P.A. Values of natural and human-made wetlands: A meta-analysis. *Water Resour. Res.* **2010**, *46*, 1–12. [[CrossRef](#)]
31. Xu, F.; Luo, M. Changes of concurrent drought and heat extremes in the arid and semi-arid regions of China during 1961–2014. *Atmos. Sci. Lett.* **2019**, *20*, e947. [[CrossRef](#)]
32. Chen, L.; Ma, Z.G.; Zhao, T.B. Modeling and analysis of the potential impacts on regional climate due to vegetation degradation over arid and semi-arid regions of China. *Clim. Change* **2017**, *144*, 461–473. [[CrossRef](#)]
33. Mao, D.H.; Wang, Z.M.; Wu, B.F.; Zeng, Y.; Luo, L.; Zhang, B. Land degradation and restoration in the arid and semiarid zones of China: Quantified evidence and implications from satellites. *Land Degrad. Dev.* **2018**, *29*, 3841–3851. [[CrossRef](#)]
34. Li, H.; Wang, J.; Zhang, J.; Qin, F.; Hu, J.; Zhou, Z. Analysis of characteristics and driving factors of wetland landscape pattern change in Henan Province from 1980 to 2015. *Land* **2021**, *10*, 564. [[CrossRef](#)]
35. Hu, W.; Li, G.; Li, Z. Spatial and temporal evolution characteristics of the water conservation function and its driving factors in regional lake wetlands—Two types of homogeneous lakes as examples. *Ecol. Indic.* **2021**, *130*, 108069. [[CrossRef](#)]
36. Wen, L.; Li, Z. Driving forces of national and regional CO₂ emissions in China combined IPAT-E and PLS-SEM model. *Sci. Total Environ.* **2019**, *690*, 237–247. [[CrossRef](#)]
37. Hu, R.; Wang, Y.; Chang, J.; Istanbuluoglu, E.; Guo, A.; Meng, X.; Li, Z.; He, B.; Zhao, Y. Coupling water cycle processes with water demand routes of vegetation using a cascade causal modeling approach in arid inland basins. *Sci. Total Environ.* **2022**, *840*, 156492. [[CrossRef](#)]
38. Wei, Y.G.; Zhu, X.H.; Li, Y.; Yao, T.; Tao, Y. Influential factors of national and regional CO₂ emission in China based on combined model of DPSIR and PLS-SEM. *J. Clean. Prod.* **2019**, *212*, 698–712. [[CrossRef](#)]
39. Hair, J.F.; Risher, J.J.; Sarstedt, M.; Ringle, C.M. When to use and how to report the results of PLS-SEM. *Eur. Bus. Rev.* **2019**, *31*, 2–24. [[CrossRef](#)]
40. Fotheringham, A.S.; Brunson, C.; Charlton, M. *Geographically Weighted Regression: The Analysis of Spatially Varying Relationships*; John Wiley & Sons: Hoboken, NJ, USA, 2003.
41. Li, S.J.; Zhou, C.S.; Wang, S.J.; Gao, S.; Liu, Z.T. Spatial Heterogeneity in the Determinants of Urban Form: An Analysis of Chinese Cities with a GWR Approach. *Sustainability* **2019**, *11*, 479. [[CrossRef](#)]
42. Ouyang, Z.; Zheng, H.; Xiao, Y.; Polasky, S.; Liu, J.; Xu, W.; Wang, Q.; Zhang, L.; Xiao, Y.; Rao, E.; et al. Improvements in ecosystem services from investments in natural capital. *Science* **2016**, *352*, 1455–1459. [[CrossRef](#)]
43. Wang, Z.M.; Wu, J.G.; Madden, M.; Mao, D.H. China's Wetlands: Conservation Plans and Policy Impacts. *Ambio* **2012**, *41*, 782–786. [[CrossRef](#)]
44. Committee, C.C.; Council, S. *The Decision on Accelerating the Reform and Development of Water Conservancy*; People's Publishing House Beijing: Beijing, China, 2010.
45. Liu, J.G.; Zang, C.F.; Tian, S.Y.; Liu, J.G.; Yang, H.; Jia, S.F.; You, L.Z.; Liu, B.; Zhang, M. Water conservancy projects in China: Achievements, challenges and way forward. *Glob. Environ. Chang.* **2013**, *23*, 633–643. [[CrossRef](#)]
46. Wu, Y.; Guo, L.D.; Xia, Z.A.; Jing, P.R.; Chunyu, X.Z. Reviewing the Poyang Lake Hydraulic Project Based on Humans' Changing Cognition of Water Conservancy Projects. *Sustainability* **2019**, *11*, 2605. [[CrossRef](#)]
47. Li, D.J.; Xu, D.Y.; Wang, Z.Y.; Ding, X.; Song, A.L. Ecological compensation for desertification control: A review. *J. Geogr. Sci.* **2018**, *28*, 367–384. [[CrossRef](#)]
48. Aliat, T.; Kaabeche, M.; Khomri, H.; Nouri, L.; Neffar, S.; Chenchouni, H. A Pedological Characterisation of Some Inland Wetlands and Ramsar Sites in Algeria. *Land Degrad. Dev.* **2016**, *27*, 693–705. [[CrossRef](#)]
49. Zhao, Y.; Wang, G.; Zhao, M.; Wang, M.; Jiang, M. Direct and indirect effects of soil salinization on soil seed banks in salinizing wetlands in the Songnen Plain, China. *Sci. Total Environ.* **2022**, *819*, 152035. [[CrossRef](#)]
50. Wu, X.; Xia, J.; Zhan, C.S.; Jia, R.L.; Li, Y.; Qiao, Y.F.; Zou, L. Modeling soil salinization at the downstream of a lowland reservoir. *Hydrol. Res.* **2019**, *50*, 1202–1215. [[CrossRef](#)]
51. Mikula, K.; Izydorczyk, G.; Skrzypczak, D.; Mironiuk, M.; Moustakas, K.; Witek-Krowiak, A.; Chojnacka, K. Controlled release micronutrient fertilizers for precision agriculture—A review. *Sci. Total Environ.* **2020**, *712*, 136365. [[CrossRef](#)]
52. Lai, Y.; Zhang, J.; Song, Y.; Cao, Y. Comparative analysis of different methods for extracting water body area of miyun reservoir and driving forces for nearly 40 years. *J. Indian Soc. Remote Sens.* **2020**, *48*, 451–463. [[CrossRef](#)]
53. Wu, X.; Gong, W.; Xu, Y. Analysis of Urban Wetland Changes and their Driving Forces based on RS and GIS: A Case Study in the Longfeng Wetland Natural Reserve, China. *Nat. Environ. Pollut. Technol.* **2016**, *15*, 377.
54. Cui, L.L.; Li, G.S.; Chen, Y.H.; Li, L.J. Response of Landscape Evolution to Human Disturbances in the Coastal Wetlands in Northern Jiangsu Province, China. *Remote Sens.* **2021**, *13*, 2030. [[CrossRef](#)]
55. Ouyang, N.L.; Li, G.S.; Cui, L.L.; Liao, H.J. Main Features and Problems of Modern Evolution Process of Coastal Wetlands in North Jiangsu, China. *J. Indian Soc. Remote Sens.* **2018**, *46*, 655–666. [[CrossRef](#)]
56. Qingguang, L. Dynamic degradation of the alpine-cold wetland and analysis of driving forces in Maqu, China. *Nat. Environ. Pollut. Technol.* **2016**, *15*, 457.
57. Gou, Q.; Qu, J.; Wang, G.; Xiao, J.; Pang, Y. Progress of wetland researches in arid and semi-arid regions in China. *Arid. Zone Res.* **2015**, *32*, 213–220.
58. Guo, H.; Pu, M.M. Local Legislation of Wetland Conservation in Xinjiang: Experience and implication. *Trib. Soc. Sci. Xinjiang* **2023**, *1*, 38–45.

59. Hayashi, M.; van der Kamp, G.; Rosenberry, D.O. Hydrology of Prairie Wetlands: Understanding the Integrated Surface-Water and Groundwater Processes. *Wetlands* **2016**, *36*, S237–S254. [[CrossRef](#)]
60. Wu, Q.S.; Lane, C.R. Delineation and Quantification of Wetland Depressions in the Prairie Pothole Region of North Dakota. *Wetlands* **2016**, *36*, 215–227. [[CrossRef](#)]
61. Liu, J.; Fang, P.; Que, Y.; Zhu, L.J.; Duan, Z.; Tang, G.; Liu, P.; Ji, M.; Liu, Y. A dataset of lake-catchment characteristics for the Tibetan Plateau. *Earth Syst. Sci. Data* **2022**, *14*, 3791–3805. [[CrossRef](#)]
62. Xu, T.; Weng, B.; Yan, D.; Wang, K.; Li, X.; Bi, W.; Li, M.; Cheng, X.; Liu, Y. Wetlands of International Importance: Status, Threats, and Future Protection. *Int. J. Environ. Res. Public Health* **2019**, *16*, 1818. [[CrossRef](#)]
63. Gao, X.; Zhao, D.; Zheng, D. Regional Differences in Surface Temperature Variation in China from 1961 to 2018. *Chin. J. Atmos. Sci.* **2023**, *47*, 995–1006. [[CrossRef](#)]
64. Bian, H.; Li, W.; Li, Y.; Ren, B.; Niu, Y.; Zeng, Z. Driving forces of changes in China’s wetland area from the first (1999–2001) to second (2009–2011) National Inventory of Wetland Resources. *Glob. Ecol. Conserv.* **2020**, *21*, e00867. [[CrossRef](#)]
65. Zhao, D.; He, H.S.; Wang, W.J.; Wang, L.; Du, H.; Liu, K.; Zong, S. Predicting wetland distribution changes under climate change and human activities in a mid-and high-latitude region. *Sustainability* **2018**, *10*, 863. [[CrossRef](#)]
66. Gong, Z.; Li, H.; Zhao, W.; Gong, H. Driving forces analysis of reservoir wetland evolution in Beijing during 1984–2010. *J. Geogr. Sci.* **2013**, *23*, 753–768. [[CrossRef](#)]
67. Kirwan, M.L.; Guntenspergen, G.R. Feedbacks between inundation, root production, and shoot growth in a rapidly submerging brackish marsh. *J. Ecol.* **2012**, *100*, 764–770. [[CrossRef](#)]
68. Nyman, J.A.; Carlross, M.; DeLaune, R.; Patrick, W., Jr. Erosion rather than plant dieback as the mechanism of marsh loss in an estuarine marsh. *Earth Surf. Process. Landf.* **1994**, *19*, 69–84. [[CrossRef](#)]
69. Turner, R.E.; Swenson, E.M.; Milan, C.S.; Lee, J.M.; Oswald, T.A. Below-ground biomass in healthy and impaired salt marshes. *Ecol. Res.* **2004**, *19*, 29–35. [[CrossRef](#)]
70. Hardy, T.; Wu, W.; Peterson, M.S. Analyzing spatial variability of drivers of coastal wetland loss in the northern Gulf of Mexico using Bayesian multi-level models. *Gisci. Remote Sens.* **2021**, *58*, 831–851. [[CrossRef](#)]
71. Doichinova, V.; Zhiyanski, M.; Hursthouse, A. Impact of urbanisation on soil characteristics. *Environ. Chem. Lett.* **2006**, *3*, 160–163. [[CrossRef](#)]
72. Ikemi, H. Geologically constrained changes to landforms caused by human activities in the 20th century: A case study from Fukuoka Prefecture, Japan. *Appl. Geogr.* **2017**, *87*, 115–126. [[CrossRef](#)]
73. Migoń, P.; Latocha, A. Human impact and geomorphic change through time in the Sudetes, Central Europe. *Quat. Int.* **2018**, *470*, 194–206. [[CrossRef](#)]
74. Werner, B.A.; Johnson, W.C.; Guntenspergen, G.R. Evidence for 20th century climate warming and wetland drying in the North American Prairie Pothole Region. *Ecol. Evol.* **2013**, *3*, 3471–3482. [[CrossRef](#)] [[PubMed](#)]
75. Fensholt, R.; Langanke, T.; Rasmussen, K.; Reenberg, A.; Prince, S.D.; Tucker, C.; Scholes, R.J.; Le, Q.B.; Bondeau, A.; Eastman, R. Greenness in semi-arid areas across the globe 1981–2007—An Earth Observing Satellite based analysis of trends and drivers. *Remote Sens. Environ.* **2012**, *121*, 144–158. [[CrossRef](#)]
76. Chen, H.; Zhao, Y. Evaluating the environmental flows of China’s Wolonghu wetland and land use changes using a hydrological model, a water balance model, and remote sensing. *Ecol. Model.* **2011**, *222*, 253–260. [[CrossRef](#)]
77. Gxokwe, S.; Dube, T.; Mazvimavi, D. Multispectral Remote Sensing of Wetlands in Semi-Arid and Arid Areas: A Review on Applications, Challenges and Possible Future Research Directions. *Remote Sens.* **2020**, *12*, 4190. [[CrossRef](#)]
78. Cuevas, J.; Daliakopoulos, I.N.; del Moral, F.; Hueso, J.J.; Tsanis, I.K. A review of soil-improving cropping systems for soil salinization. *Agronomy* **2019**, *9*, 295. [[CrossRef](#)]
79. Huang, J.P.; Ma, J.R.; Guan, X.D.; Li, Y.; He, Y.L. Progress in Semi-arid Climate Change Studies in China. *Adv. Atmos. Sci.* **2019**, *36*, 922–937. [[CrossRef](#)]
80. Meng, W.Q.; He, M.X.; Hu, B.B.; Mo, X.Q.; Li, H.Y.; Liu, B.Q.; Wang, Z.L. Status of wetlands in China: A review of extent, degradation, issues and recommendations for improvement. *Ocean Coast. Manag.* **2017**, *146*, 50–59. [[CrossRef](#)]

Disclaimer/Publisher’s Note: The statements, opinions and data contained in all publications are solely those of the individual author(s) and contributor(s) and not of MDPI and/or the editor(s). MDPI and/or the editor(s) disclaim responsibility for any injury to people or property resulting from any ideas, methods, instructions or products referred to in the content.